IEEE Access
Multidisciplinary : Rapid Review : Open Access Journal

Received March 23, 2021, accepted April 1, 2021, date of publication April 13, 2021, date of current version April 27, 2021.

Digital Object Identifier 10.1109/ACCESS.2021.3073082

A Novel Formulation to Compute Sensitivities to Solve Congestions and Voltage Problems in Active Distribution Networks

FCO. JAVIER ZARCO-SOTO, JOSÉ L. MARTÍNEZ-RAMOS, (Senior Member, IEEE), AND PEDRO J. ZARCO-PERIÑÁN

Departamento de Ingeniería Eléctrica, Escuela Técnica Superior de Ingeniería, Universidad de Sevilla, 41092 Sevilla, Spain

Corresponding author: Fco. Javier Zarco-Soto (fjzarco@outlook.com)

This work was supported in part by the European Union's Horizon 2020 Research and Innovation Program under Agreement 764090, and in part by the CERVERA Research Program of CDTI, the Industrial and Technological Development Centre of Spain, through the Research Project HySGrid+ under Grant CER-20191019.

ABSTRACT Sensitivities are broadly appreciated because of its simplicity and good results in solving voltage problems and congestions in transmission networks. However, since sensitivity calculation is based on a linear approximation of the power flow equations, all decisions commit an intrinsic error that might lead into unexpected results, especially in distribution networks. This paper analyzes the error associated to sensitivities considering a wide range of control variables and proposes a novel formulation to extend the use of sensitivities to manage congestions in active distribution networks. First, a theoretical analysis is performed to study the origin and propagation of errors. Then, numerical results are presented for two types of distribution networks (20 kV and low voltage grids). Finally, a novel formulation is proposed to extend the use of sensitivities to manage congestions, which will allow to reuse previous sensitivity-based methodologies to solve both voltage problems and congestions in active distribution networks.

INDEX TERMS Sensitivities, sensitivity-based methods, voltage control, congestion management, distribution networks, renewable energy sources.

I. INTRODUCTION

The development of modern life directly relies on energy consumption that is still mainly based on fossil fuels [1], which is responsible of most greenhouse gas emissions. The growing concern of society has led to promulgate new laws and recommendations [2]–[5] to promote the use of renewable energy sources (RES) and enhance resource efficiency. The fact that RES has become the most appropriate solution to replace inefficient fossil fuel technologies is challenging the current electric system. Part of this generation is still being grouped and connected at transmission networks, i.e. offshore wind farms; however, the modularity and emission-free characteristics allow to install distributed RES (DRES) within distribution networks, close to end users. Traditionally, only passive loads were connected to these systems and it could be assumed that power flows were unidirectional, from the point of interconnection with the transmission system to downstream. However, distribution networks are pivoting to become active because of the increasing penetration of DRES and, consequently, the classical operation is affected [6], [7]. Power flows become bidirectional since generation excess may be fed back to the upstream system [8], e.g. during midday due to photovoltaic generation. As a result, the traditional voltage profile is significantly modified since the voltage at intermediate nodes may be higher than at the connection buses with higher voltage networks. On the other hand, increasing generation in conjunction to novel heavy loads, as plug-in electric vehicles, may lead to line and transformer congestions if no remedial actions are implemented.

Voltage has been traditionally controlled in distribution networks through the on-load tap changing (OLTC) transformers that feed the system, whilst placing shunt capacitors at the substations was used to compensate the reactive power demand [6], [9]. Regarding congestion management, lines and transformers were usually dimensioned to supply the maximum demand considering future variations and, therefore, no further supervision nor control was required.

The associate editor coordinating the review of this manuscript and approving it for publication was Hazlie Mokhlis.

The new paradigm difficult distribution system operation that becomes as complex as transmission operation, and new initiatives are being proposed to tackle the emerging problems. For instance, distribution networks may also need to combine day-ahead scheduling with real-time dispatch [10] as in transmission. Besides, some authors point out that coordinated actions between both operators would allow to achieve effective and efficient voltage control and congestion management [11] as well as regulate active and reactive power exchange at frontier nodes [12], [13] to guarantee security, reliability, and cost-efficiency. However, the high number of DRES, which may be spread, pose a challenge to traditional systems [14]. In that sense, new forms of distributed active management are increasingly proposed [15].

Among the initiatives proposed to solve voltage problems, linearizing the system model to compute sensitivities stands out for its simplicity and good results. A metaheuristic sensitivity-based algorithm is proposed in [16] that combines rules with numerical algorithms to calculate sensitivities. The developed tool determines the most appropriate actions considering contingencies, network constraints and costs. Sensitivities are used in [17] to speed up the resolution of a volt/var control problem through a variant of the discrete coordinate-descent algorithm, whereas [18] presents a toolkit to simplify the development of sensitivity-based voltage strategies by computing sensitivities through a perturb-and-observe algorithm. Furthermore, local sensitivity analyses are used in [19] for voltage regulation at the nodes where distributed wind turbines are connected. The decentralized control considers the capability constraints of wind turbines and acts on the active and reactive power injected by these DRES to avoid disconnections. On the other hand, sensitivities can also be used for determining the maximum DRES generation beforehand [20]. The methodology proposed allows to consider voltage limits and avoid performing repetitive power flow studies.

Regarding congestion management, the techniques currently used consists of network reconfiguration, active power control, reactive power control and market-based methods [21]. Reconfiguration of the network needs for telecontrol to connect or disconnect lines; however, this is not always possible since distribution systems are not so automated as transmission networks. For instance, the method proposed in [22] corrects line congestions by switching lines to transfer DRES generation to other feeders as well as DRES curtailment, which is minimized. On the other hand, demand response can also be used for incentivizing users to alleviate system congestions. Ref. [23] presents a distribution congestion price to avoid possible congestions in the day-ahead market. Another approach is presented in [24], where the sensitivity of severity indexes is used for solving overloads considering both DRES and load shedding, and their influence over the problem.

Sensitivity-based methods are appreciated for their simplicity and providing results easily with low computational cost. However, since the calculation of these sensitivities is based on a linear approximation of the power flow equations, all decisions commit an intrinsic error that might lead into unexpected results. Besides, the use of sensitivities regarding voltages is widespread in contrast to the low number of applications regarding congestion management. In that sense, the aim of this paper is twofold. Firstly, to estimate the errors associated to sensitivities. Secondly, to extend the use of sensitivities for solving congestions in distribution networks.

The major contributions of this paper are as follows. First, a theoretical error analysis is proposed which reveals that it is not possible to forecast a priori the error associated to sensitivities, nor to obtain analytical expressions for the errors. The main reason is the large number of parameters that depend on the type and state of the system. Then, a quantitative analysis is performed to estimate the error of each sensitivity according to network characteristics. Finally, it is proposed to extend the use of sensitivities to solve congestions in lines and transformers along with voltage problems. A novel formulation is proposed that leads into much better results.

The remainder of the text is organized as follows. Section 2 analyzes theoretically the origin and propagation of the associated error to every sensitivity matrix. Then, in Section 3 numerical results are given and discussed for two different distribution networks. New sensitivities are analyzed in Section 4 in order to extend the use of sensitivities to consider congestions, and a new formulation is proposed. Finally, Section 5 presents the conclusions of this study.

II. ANALYSIS OF THE ERRORS ASSOCIATED TO THE USE OF SENSITIVITIES

Sensitivity-based methodologies rely on the information provided by sensitivities about how controls affect to each electrical magnitude that is considered. The more accurate sensitivities are, the more precise the results will be. In addition, as sensitivity matrices are obtained for certain operating state, wider variations lead into greater errors.

Prior to the study, the sensitivity matrices that are used must be defined. On the one hand, control actions available to correct voltages and congestions are the ones that already exist in traditional networks along with those introduced in new active distribution networks:

- OLTC transformers.
- Shunt capacitors.
- RES (e.g. photovoltaic and wind plants).
- DRES (e.g. rooftop photovoltaics).
- Energy storage systems.
- Virtual power plants.
- Microgrids.
- Demand response (including direct load control, power curtailment and load shedding).
- Plug-in electric vehicle coordinated charging and discharging.

OLTC transformers modify the turns ratio between the two nodes where the machine connects, whereas shunt capacitors vary the reactive power injected at demand nodes, where voltage is not controlled.

Distributed or not renewable generators, energy storage systems, virtual power plants and microgrids allow to control the active power, the reactive power, or the voltage at the point of interconnection depending on their control algorithms. In [25] the operation of power converters is classified into three groups: grid-feeding, grid-supporting and grid-forming. The former is oriented to deliver power at an energized and typically robust system, whereas the latter is designed to set the voltage amplitude and frequency locally. The grid-supporting mode is between the other two and its purpose is to contribute to control the grid frequency and voltages by means of delivering adequate values of active and reactive power. Therefore, RES, DRES, energy storage systems, virtual power plants and microgrids will be able to control the voltage setpoint, the active or the reactive power injected at the interconnection node according to the technology implemented.

In order to enable consumers to vary its power consumption to meet system needs, demand response is used. It allows to offer competitive prices not only to reduce the peak and occasional demand spikes, but also to avoid and solve system problems [26]. Demand response includes direct load control, power curtailment and load shedding under extreme situations [27] where other control variables are unavailable or insufficient to solve system problems.

Similarly, plug-in electric vehicles may also be considered. If charging is left uncontrolled, plug-in electric vehicles can be considered as heavy mobile loads. Due to its inherent random space-time characteristic, they are difficult to predict and control accurately, which affect negatively power quality and may cause voltage and current problems [28]. However, plug-in electric vehicles can also be considered as energy storage systems that provide the grid operation with flexibility through vehicle-to-grid technology.

On the other hand, the operational constraints of the network must be considered to determine the best control actions to solve voltage problems and congestions. Otherwise, new limit violations could be created in nodes, lines or transformers, or the current problems may be worsened after taking corrective actions. The operational limits considered in this study are listed below.

- Voltages at demand nodes, which are not controlled by any element.
- Reactive power of DRES, RES, storage devices, virtual power plants and microgrids that maintain the voltage setpoint at one node.
- Current that circulates through lines and transformers.

Therefore, the sensitivity matrices that are calculated provide the linear relationship between control variables and dependent variables subject to operational limits, which include the voltages and congestions that should be corrected.

From the point of view of sensitivities, control variables are grouped according to the electrical magnitude they modify: active power injected at demand and generation nodes (P), reactive power injected at demand nodes (Q_D), voltage at generation nodes (V_G) and transformer taps (t). Similarly, dependent variables subject to operational limits can be classified considering the electrical magnitude they refer to: voltage at demand nodes (V_D), reactive power at generation nodes (Q_G) and current through lines and transformers (I). It is worth mentioning that this classification is related to the classical one of the Load Flow Problem [29], e.g. at PV nodes both P and V_G may be modified, but not the reactive power since it is used for achieving the desired voltage value. Also, note that subscript D refers to demand nodes and G to generation nodes.

Once the sensitivity matrices are obtained, it is possible to calculate control actions to correct a violation of the operational limits [16], [32], [33]. For example, if a voltage is below the lower limit by an amount ΔV_D, the most efficient control action to correct it can be determined, as well as its amount, e.g. an increase in the reactive power injected by a capacitor bank, ΔQ_D. Note that the model of the power system, including demands and the renewable generations, must be updated as often as necessary to capture the changes due to the evolution of the state of the power system over time. Likewise, the power delivered by a renewable generator, as well as its voltage, affect the operational limits of the generator (e.g. the reactive power that it can supply), so its values must be updated to obtain feasible control actions.

Sensitivity calculation is based on linearizing the power flow equations at the current operating state. Then, by assuming that only one control action is taken at the same time, a set of expressions for every matrix is deduced [16].

First, the well-known power flow equations are written as follows [29].

$$P_i = V_i \sum_{j=1}^{n} V_j \left(G_{ij}(t)\, cos\theta_{ij} + B_{ij}(t)\, sin\theta_{ij} \right) \tag{1}$$

$$Q_i = V_i \sum_{j=1}^{n} V_j \left(G_{ij}(t)\, sin\theta_{ij} - B_{ij}(t)\, cos\theta_{ij} \right) \tag{2}$$

where P_i and Q_i denote the active and reactive power at node i, respectively; V_i and V_j the voltage amplitude at nodes i and j, respectively; G_{ij} and B_{ij} the conductance and the susceptance between nodes i and j, respectively; θ_{ij} the phase angle difference between nodes i and j; n the number of nodes. Note that both G_{ij} and B_{ij} can depend on transformer taps that modify the turns ratio, t.

For a single line or transformer connected between nodes i and j, the current leaving i is calculated as

$$\begin{aligned} I_{ij}^2 = {} & V_i^2 \left(\left(g_{ij} + g_{s_i} \right)^2 + \left(b_{ij} + b_{s_i} \right)^2 \right) + V_j^2 \left(g_{ij}^2 + b_{ij}^2 \right) \\ & + 2 V_i V_j \left(-cos\theta_{ij} \left(g_{ij}^2 + b_{ij}^2 + g_{s_i} g_{ij} + b_{s_i} b_{ij} \right) \right. \\ & \left. + sen\theta_{ij} \left(-g_{s_i} b_{ij} + b_{s_i} g_{ij} \right) \right) \end{aligned} \tag{3}$$

where g_{ij} and b_{ij} are the series conductance and susceptance between nodes i and j, respectively; g_{s_i} and b_{s_i} the shunt conductance and susceptance at node i, respectively. In case of transformers, both g_{ij} and b_{ij} depend on transformer taps. Note that I^2 is used to avoid working with square roots.

Power flow equations can be represented by their Taylor Series evaluated at the operating state as two polynomial functions that consist of the infinite sum of derivative terms. In order to linearize the power flow equations, only first order terms are considered. Additionally, and to meet the previous classification of control variables and operational limits, voltages and reactive powers are grouped according to the type of node, i.e. demand and generation nodes. Reactive power at demand nodes, Q_D, is known in contrast to the voltage, V_D, which remains unknown until the state is solved. On the contrary, reactive power at generation nodes, Q_G, is used to maintain voltages, V_G, at a reference value. In that sense, control variables are the independent variables to be defined (P, Q_D, V_G, t), so that operational limits (V_D, Q_G, I^2) are met, which are the dependent variables to be controlled.

Therefore, the resulting approximated expressions of equations (1) – (3) are presented as follows in matrix form.

$$\begin{bmatrix} \Delta P \\ \Delta Q_D \\ \Delta Q_G \\ \Delta I^2 \end{bmatrix} \approx \begin{bmatrix} \frac{\partial P}{\partial \theta} & \frac{\partial P}{\partial V_D} & \frac{\partial P}{\partial V_G} & \frac{\partial P}{\partial t} \\ \frac{\partial Q_D}{\partial \theta} & \frac{\partial Q_D}{\partial V_D} & \frac{\partial Q_D}{\partial V_G} & \frac{\partial Q_D}{\partial t} \\ \frac{\partial Q_G}{\partial \theta} & \frac{\partial Q_G}{\partial V_D} & \frac{\partial Q_G}{\partial V_G} & \frac{\partial Q_G}{\partial t} \\ \frac{\partial I^2}{\partial \theta} & \frac{\partial I^2}{\partial V_D} & \frac{\partial I^2}{\partial V_G} & \frac{\partial I^2}{\partial t} \end{bmatrix} \begin{bmatrix} \Delta \theta \\ \Delta V_D \\ \Delta V_G \\ \Delta t \end{bmatrix} \tag{4}$$

Sensitivity matrices can be then obtained by operating adequately.

For illustration purposes, the matrix that relates Q_D with V_D is calculated. From equation (4), it is stated that:

$$\Delta P \approx \frac{\partial P}{\partial \theta}\Delta\theta + \frac{\partial P}{\partial V_D}\Delta V_D + \frac{\partial P}{\partial V_G}\Delta V_G + \frac{\partial P}{\partial t}\Delta t \tag{5}$$

$$\Delta Q_D \approx \frac{\partial Q_D}{\partial \theta}\Delta\theta + \frac{\partial Q_D}{\partial V_D}\Delta V_D + \frac{\partial Q_D}{\partial V_G}\Delta V_G + \frac{\partial Q_D}{\partial t}\Delta t \tag{6}$$

As previously mentioned, it is assumed that only one control action is taken at the same time, in other words, when a control variable is modified the others remain constant. Since in this example Q_D is the control variable, equations (5) and (6) can be thus simplified considering the change of the rest of the variables null, i.e. $\Delta P = \Delta V_G = \Delta t = 0$. Finally, it is possible to solve $\Delta\theta$ from (5) and use it in (6) to obtain the following expression.

$$\Delta V_D = S_{V_D,Q_D}\Delta Q_D \tag{7}$$

where S_{V_D,Q_D} is the sensitivity matrix that relates the reactive power injected at demand nodes to the voltages also at demand nodes. The corresponding expression is as follows.

$$S_{V_D,Q_D} = \left\{ \frac{\partial Q_D}{\partial V_D} - \frac{\partial Q_D}{\partial \theta}\left[\frac{\partial P}{\partial \theta}\right]^{-1}\frac{\partial P}{\partial V_D} \right\}^{-1} \tag{8}$$

The following sensitivity matrices, which are used in this study, can be obtained in a similar way by considering the proper equations and assumptions. The expressions regarding V_D are:

$$S_{V_D,P} = \left\{ \frac{\partial Q_D}{\partial \theta}\left[\frac{\partial P}{\partial \theta}\right]^{-1}\frac{\partial P}{\partial V_D} - \frac{\partial Q_D}{\partial V_D} \right\}^{-1} \frac{\partial Q_D}{\partial \theta}\left[\frac{\partial P}{\partial \theta}\right]^{-1} \tag{9}$$

$$S_{V_D,V_G} = -S_{V_D,Q_D}\left\{ \frac{\partial Q_D}{\partial V_G} - \frac{\partial Q_D}{\partial \theta}\left[\frac{\partial P}{\partial \theta}\right]^{-1}\frac{\partial P}{\partial V_G} \right\} \tag{10}$$

$$S_{V_D,t} = -S_{V_D,Q_D}\left\{ \frac{\partial Q_D}{\partial t} - \frac{\partial Q_D}{\partial \theta}\left[\frac{\partial P}{\partial \theta}\right]^{-1}\frac{\partial P}{\partial t} \right\} \tag{11}$$

The sensitivity matrices for reactive power at generation nodes, Q_G, are written as follows.

$$S_{Q_G,Q_D} = \left\{ \frac{\partial Q_G}{\partial V_D} - \frac{\partial Q_G}{\partial \theta}\left[\frac{\partial P}{\partial \theta}\right]^{-1}\frac{\partial P}{\partial V_D} \right\} S_{V_D,Q_D} \tag{12}$$

$$S_{Q_G,P} = \frac{\partial Q_G}{\partial \theta}\left[\frac{\partial P}{\partial \theta}\right]^{-1} - \frac{\partial Q_G}{\partial \theta}\left[\frac{\partial P}{\partial \theta}\right]^{-1}\frac{\partial P}{\partial V_D}S_{V_D,P} + \frac{\partial Q_G}{\partial V_D}S_{V_D,P} \tag{13}$$

$$S_{Q_G,V_G} = -\frac{\partial Q_G}{\partial \theta}\left[\frac{\partial P}{\partial \theta}\right]^{-1}\frac{\partial P}{\partial V_D}S_{V_D,V_G} - \frac{\partial Q_G}{\partial \theta}\left[\frac{\partial P}{\partial \theta}\right]^{-1}\frac{\partial P}{\partial V_G} + \frac{\partial Q_G}{\partial V_D}S_{V_D,V_G} + \frac{\partial Q_G}{\partial V_G} \tag{14}$$

$$S_{Q_G,t} = -\frac{\partial Q_G}{\partial \theta}\left[\frac{\partial P}{\partial \theta}\right]^{-1}\frac{\partial P}{\partial V_D}S_{V_D,t} - \frac{\partial Q_G}{\partial \theta}\left[\frac{\partial P}{\partial \theta}\right]^{-1}\frac{\partial P}{\partial t} + \frac{\partial Q_G}{\partial V_D}S_{V_D,t} + \frac{\partial Q_G}{\partial t} \tag{15}$$

Regarding the sensitivity matrices for the current through lines and transformers, I^2:

$$S_{I^2,Q_D} = \left\{ \frac{\partial I^2}{\partial V_D} - \frac{\partial I^2}{\partial \theta}\left[\frac{\partial P}{\partial \theta}\right]^{-1}\frac{\partial P}{\partial V_D} \right\} S_{V_D,Q_D} \tag{16}$$

$$S_{I^2,P} = \frac{\partial I^2}{\partial \theta}\left[\frac{\partial P}{\partial \theta}\right]^{-1} - \frac{\partial I^2}{\partial \theta}\left[\frac{\partial P}{\partial \theta}\right]^{-1}\frac{\partial P}{\partial V_D}S_{V_D,P} + \frac{\partial I^2}{\partial V_D}S_{V_D,P} \tag{17}$$

$$S_{I^2,V_G} = -\frac{\partial I^2}{\partial \theta}\left[\frac{\partial P}{\partial \theta}\right]^{-1}\frac{\partial P}{\partial V_D}S_{V_D,V_G} - \frac{\partial I^2}{\partial \theta}\left[\frac{\partial P}{\partial \theta}\right]^{-1}\frac{\partial P}{\partial V_G} + \frac{\partial I^2}{\partial V_D}S_{V_D,V_G} + \frac{\partial I^2}{\partial V_G} \tag{18}$$

$$S_{I^2,t} = -\frac{\partial I^2}{\partial \theta}\left[\frac{\partial P}{\partial \theta}\right]^{-1}\frac{\partial P}{\partial V_D}S_{V_D,t} - \frac{\partial I^2}{\partial \theta}\left[\frac{\partial P}{\partial \theta}\right]^{-1}\frac{\partial P}{\partial t} + \frac{\partial I^2}{\partial V_D}S_{V_D,t} + \frac{\partial I^2}{\partial t} \tag{19}$$

It is then clear that the errors associated to the linear approximation are propagated according to the resulting expressions. As an example, the sensitivity matrix calculation in (8) can be repeated but considering the errors through each expression. Again, the non-linear terms from the Taylor series of the power flow equations are neglected and thus the initial errors are equal to these terms. In this way, equations (5) and (6) are rewritten as

$$\Delta P = \frac{\partial P}{\partial \theta}\Delta\theta + \frac{\partial P}{\partial V_D}\Delta V_D + \frac{\partial P}{\partial V_G}\Delta V_G + \frac{\partial P}{\partial t}\Delta t + \epsilon_P \tag{20}$$

$$\Delta Q_D = \frac{\partial Q_D}{\partial \theta}\Delta\theta + \frac{\partial Q_D}{\partial V_D}\Delta V_D + \frac{\partial Q_D}{\partial V_G}\Delta V_G + \frac{\partial Q_D}{\partial t}\Delta t + \epsilon_{Q_D} \tag{21}$$

where ϵ_P and ϵ_{Q_D} are the error due to linearizing the expressions of the active power and reactive power at demand nodes, respectively.

Following the same reasoning as for equations (7) and (8), it is assumed that only one control action is taken. Then, $\Delta\theta$ is solved from (20) and used in (21), leading to an analogous expression to (7):

$$\Delta V_D = S_{V_D,Q_D}\Delta Q_D + \epsilon_{S_{V_D,Q_D}} \tag{22}$$

where $\epsilon_{S_{V_D,Q_D}}$ denotes the error associated to the sensitivity matrix, which is equal to

$$\epsilon_{S_{V_D,Q_D}} = S_{V_D,Q_D}\left\{\epsilon_{Q_D} - \frac{\partial Q_D}{\partial \theta}\left[\frac{\partial P}{\partial \theta}\right]^{-1}\epsilon_P\right\} \tag{23}$$

Equation (23) is of relative importance since it allows to reach the following conclusions. On the one hand, the initial error due to linearizing the power flow equations depends on the magnitude of the non-linear terms neglected, in other words, the second- and superior-order elements. Since only one control action is taken at the same time, the other variables become null and the resulting error relies on the remaining variations along with the values of the derivative terms. In the previous example, the variables that became null were $\Delta P = \Delta V_G = \Delta t = 0$, whereas $\Delta\theta$, ΔV_D and ΔQ_D remained not equal to zero and were multiplied by their respective derivative terms. Therefore, the linearity and thus the error depends on the control variable considered.

With regards to the derivative terms, the power flow equations are functions of the voltage amplitude and angle in conjunction with line and transformer parameters, which compound the admittance matrix. In this way, the terms that are neglected also depend on these elements, which vary according to the type of network and the state of the system. The former refers to the characteristics of the grid, that is, the topology, the voltage level that affects the R/X ratio of lines, the type of conductors, the type of lines (overhead or underground), etc. The state of the system is defined according to the level of the power consumption and generation, the position of transformer taps, shunt capacitors, etc.

On the other hand, this initial error increases or decreases according to the expression of each sensitivity matrix, which is affected by the type and the number of operations required along with the first-order derivatives involved. In addition, the latter, and thus the final error, again relies on the type of network and the state of the system.

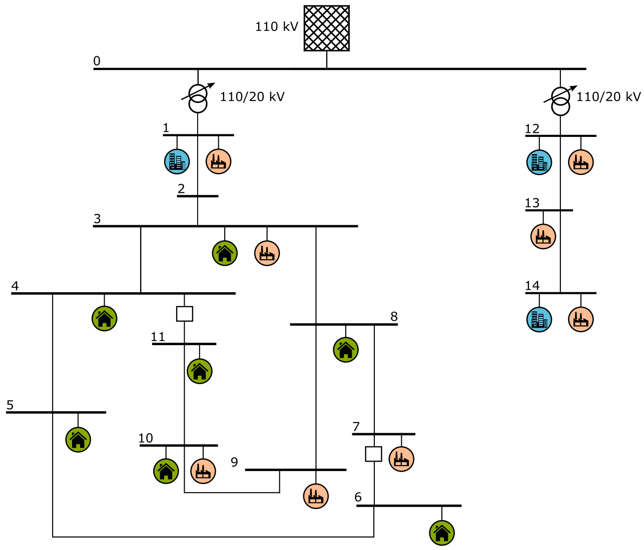

FIGURE 1. MV benchmark system.

It is worth mentioning that this analysis does not consider numerical calculation errors, especially when calculating inverse matrices.

Therefore, the theoretical error reveals that it is not possible to forecast a priori the error associated to each sensitivity matrix nor to obtain the corresponding analytical expression. The main reason is the large number of parameters that depend on the type of network and the state of the system, which is continuously changing. In order to quantify the errors, the following section presents a quantitative error analysis based on testing different control actions in two distribution networks.

III. QUANTITATIVE ERROR ANALYSIS

The purpose of the following practical error analysis is to shed light on the magnitude of the errors associated to control actions and provide insight into the adequacy of sensitivities to forecast new states after implementing corrective control actions. Within the previous section, it was demonstrated the difficulty of providing analytical error expressions, mainly because of the large number of parameters involved. In order to quantify the error, two distribution systems are studied: a medium voltage and a low voltage network.

The medium voltage (MV) system is presented in [30]. The nominal voltage is 20 kV and it is connected to a 110 kV system. As shown in Fig. 1, the network is compound of two feeders and presents both industrial and residential loads. Some of them represent large consumers as node 1, where the residential load is 15.3 MVA and the industrial is 5.1 MVA. However, other nodes only present small consumers as node 10, where the residential load is 490 kVA and the industrial load is 80 kVA. For the error analysis it is considered that there are control devices in all nodes.

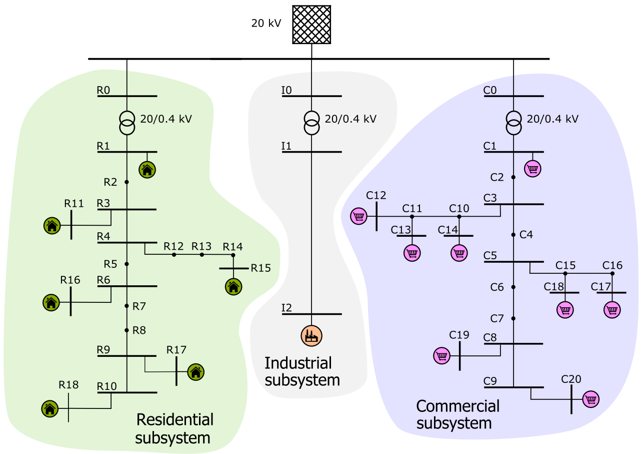

FIGURE 2. LV benchmark system.

Therefore, the control variables are both transformer taps, the voltage setpoint at node 0 and 3, where DRES are supposed to implement grid-supporting mode, reactive power injections at the remaining nodes and active power injections at all nodes except the slack bus.

With regards to the low voltage (LV) system, it is presented in [31]. The nominal voltage is 400 V and a three-phase balanced model is used. As depicted in Fig. 2, the grid is connected to a 20 kV distribution network and there are three feeders that represent residential, industrial and commercial subsystems. In LV systems it is uncommon that transformers are equipped with OLTC devices, therefore, transformer taps are not considered as a control variable. As for the medium voltage analysis, it is supposed that DRES are connected within all nodes. The available variables are thus the voltage setpoint of the 20 kV network and at node R1, where a grid-supporter DRES is supposed to be connected. Within the remaining nodes, reactive power actions are considered, whereas active power injections at all nodes are possible, except at the 20 kV network that is the slack of the LV system.

It is assumed that these benchmark networks are operated under normal conditions, that is, close to their nominal values. To study the influence of load conditions, four initial states are defined according to the maximum load (25%, 50%, 75% and 100%). Then, control variables are modified within a range from the initial states within subsequent iterations. In this way, the following methodology has been applied to both distribution systems:

1. Select one of the four initial states according to load conditions.
2. Compute the sensitivity matrices for the initial state.
3. Select one of the control variables groups (Q_D, V_G, t, P).
4. Define the range within which the control variable will be modified.
5. Modify every control through subsequent iterations according to each value in this range. In every iteration, the expected state through the sensitivity approximation and the real state by solving the power flow problem [29] are computed. Next, the relative errors are determined as the difference between the real and the expected value divided by the former. For instance, if the control variable in step 3 is transformer taps, the tap of the first transformer is modified, and the new expected and real states are computed along with the errors. The system is then returned to the initial conditions and the tap is modified again.
6. Return to 3 and choose another control variable group. The process finishes when there are no more control variables left.

At the initial state, some magnitudes present significantly different values within the available controls. In particular, the active and the reactive power injected at nodes. Distribution systems usually have different types of loads which include heavy loads that represent large consumers, such as industries, shopping centers or residential areas, and small loads associated to small or rural consumers. In that sense, a control action that decreases 100 kW the power consumption within the nodes of the system could not represent a significant percentage of the nominal load were a large consumer is connected, e.g. the 15.3 MVA residential load connected at node 1 of the MV system. However, 100 kW may be more than the maximum load of some small consumers, e.g. the 80 kVA industrial load at node 10. Such actions would go against the assumption that the new system state is not going to be far from the initial operating point, which is the base of the linearization of power flow equations. In fact, the expected new state associated to these large control actions could lead into invalid results, such as negative amplitude of the current that flows through lines or transformers and operational constraint violations like under- or overvoltage. Therefore, it will not be considered the actions that end up into invalid results or the ones that modify the active or reactive power more than the consumption at the node.

A. ERRORS ASSOCIATED TO THE USE OF SENSITIVITIES

After studying more than 300,000 control actions by applying the previous methodology to both distribution systems, the errors are computed. Within the following subsections, the relative errors of the system constraints with respect to fixed control actions are presented and discussed. In the MV network, transformer taps are modified within the range ± 5 %, whereas the active power injected is varied within the range ± 500 kW and the reactive power at demand nodes between ± 500 kvar. Since loads are smaller in the LV system, the selected ranges for this network are ± 50 kW and ± 50 kvar. In both cases, the voltage setpoint at generation nodes is varied within the range ± 5 %. Note that control actions are always taken from the initial state.

1) VOLTAGES AT DEMAND NODES

The way control variables affect voltages at demand nodes is modelled by equations (8) – (11), according to the electrical magnitude modified. Both the LV and the MV system present very good results from the point of view of voltages.

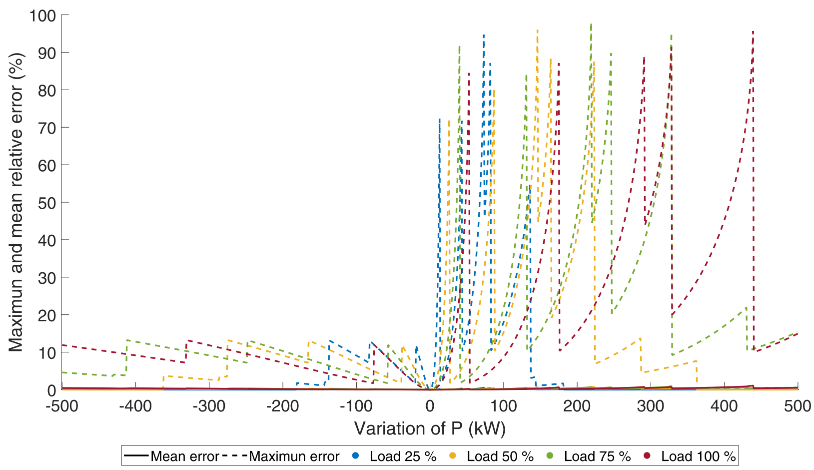

FIGURE 3. Maximum and mean relative error of the of the current through lines and transformers using the sensitivity matrix with respect to the active power, $S_{I^2,P}$.

TABLE 1. Relative errors (%) of the voltage at demand nodes: (a) MV system, and (b) LV system.

(A)

		Load level			
		25 %	*50 %*	*75 %*	*100 %*
P	***Max***	*<0.001*	*<0.001*	*<0.001*	*<0.001*
	Mean	*<0.001*	*<0.001*	*<0.001*	*<0.001*
Q_D	***Max***	*<0.001*	*<0.001*	*<0.001*	*<0.001*
	Mean	*<0.001*	*<0.001*	*<0.001*	*<0.001*
t	***Max***	*0.3*	*0.3*	*0.3*	*0.3*
	Mean	*<0.1*	*<0.1*	*<0.1*	*<0.1*
V_G	***Max***	*0.4*	*0.5*	*0.6*	*0.7*
	Mean	*<0.1*	*<0.1*	*<0.1*	*<0.1*

(B)

		Load level			
		25 %	*50 %*	*75 %*	*100 %*
P	***Max***	*<0.1*	*<0.1*	*0.1*	*0.3*
	Mean	*<0.01*	*<0.01*	*<0.01*	*<0.01*
Q_D	***Max***	*<0.01*	*<0.1*	*<0.1*	*<0.1*
	Mean	*<0.01*	*<0.001*	*<0.01*	*<0.01*
V_G	***Max***	*<0.01*	*<0.1*	*<0.1*	*<0.1*
	Mean	*<0.01*	*<0.01*	*<0.01*	*0.01*

TABLE 2. Relative errors (%) of generator reactive powers: (a) MV system, and (b) LV system.

(A)

		Load level			
		25 %	*50 %*	*75 %*	*100 %*
P	***Max***	0.02	0.2	1.7	3.5
	Mean	<0.01	0.05	0.3	1.3
Q_D	***Max***	<0.01	<0.01	0.05	1.3
	Mean	<0.01	<0.01	0.01	0.2
t	***Max***	5.5	5.1	4.6	8.0
	Mean	1.6	1.6	1.8	3.4
V_G	***Max***	11.7	15.6	13.0	11.2
	Mean	7.1	6.4	6.4	6.9

(B)

		Load level			
		25 %	*50 %*	*75 %*	*100 %*
P	***Max***	*1.0*	*2.1*	*1.9*	*1.5*
	Mean	*0.9*	*0.5*	*0.5*	*0.4*
Q_D	***Max***	*1.8*	*2.9*	*3.8*	*3.6*
	Mean	*0.6*	*1.0*	*1.9*	*1.2*
V_G	***Max***	*6.0*	*6.7*	*7.6*	*9.0*
	Mean	*2.9*	*3.1*	*3.4*	*3.8*

It is possible to achieve tiny errors even under large control actions. For instance, the errors associated to consuming or injecting reactive power in the range ±500 kvar at the MV system is less than 1 V. Such results were to be expected since sensitivity-based tools have been successfully used previously at transmission networks [32]–[34]. Table 1 present the errors with respect to the control variable group that is modified according to the above-mentioned ranges.

2) REACTIVE POWER OF GENERATORS

In this case, equations (12) – (15) define the sensitivities between control variables and the reactive power of generators. As shown in Table 2, the associated errors are higher than in the previous case. If necessary, the magnitude of control actions may be limited to avoid rocketing the associated errors.

3) CURRENT THROUGH LINES AND TRANSFORMERS

The relation between control variables and the current through lines and transformers is modelled by equations (16) – (19). As shown in Table 3, these sensitivities lead to high errors. In order to understand better these issues, the following example is used.

Fig. 3 presents the relative error of the current through lines and transformers in the MV system regarding actions on the active power injected. The colors are related to the load level used to define the initial state (25%, 50%, 75% and 100%), whereas the continuous lines represent the mean error and the dashed lines the maximum error among all lines and transformers. Note that the discontinuities are caused by invalid results as previously explained, e.g. actions on the active power that exceed the consumption at the node it

TABLE 3. Relative errors (%) of current through lines and transformers: (a) MV system, and (b) LV system.

(A)

		Load level			
		25 %	50 %	75 %	100 %
P	Max	94.7	96.0	98.0	95.7
	Mean	0.6	0.8	0.9	1.1
Q_D	Max	17.9	21.8	21.8	21.8
	Mean	0.1	0.1	0.2	0.2
t	Max	87.2	94.9	94.6	90.0
	Mean	4.2	5.7	5.2	3.9
V_G	Max	87.8	94.7	94.6	91.9
	Mean	9.4	9.1	6.6	5.3

(B)

		Load level			
		25 %	50 %	75 %	100 %
P	Max	92.5	86.7	83.1	97.1
	Mean	1.9	1.8	1.9	2.3
Q_D	Max	21.4	21.9	23.3	21.3
	Mean	0.6	0.6	1.2	0.6
V_G	Max	97.9	99.1	98.2	72.2
	Mean	1.8	1.9	2.0	1.6

takes place. It can be observed in Fig. 3 that, although the mean error is acceptable, the maximum error is too high.

As for example, when loads are at their nominal value (red) and the active power is subsequently modified 175 kW as previously explained, the mean error obtained after studying the current amplitude through all lines and transformers is adequate. However, the maximum error rockets to 87 %, that means, the sensitivity matrix does not work properly in some cases. This maximum error comes from line 11 – 10 when increasing the active power generation (or decreasing the demand) at node 11.

The main reason for this large error is the fact that line 11 – 10 is relatively unloaded and close to the node where the action is taken, that is, highly sensitive. If the action considered decreases the current through the line, it will be reduced until the node becomes net generator. Then, the current amplitude through the line will increase but the phasor of the current will be in the opposite quadrant, as shown in Fig. 4a. Initially, the total consumption at node 11 was 331 kW and 83 kvar, that is, 341 kVA or 10 A. Since the line is short, power losses are negligible, and 10 A circulated in the initial state. After increasing 175 kW the generation, the net power consumption becomes 177 kVA or 5 A. In Fig. 4b it is shown the linear approximation by the sensitivity matrix $S_{I^2,P}$, which corresponds to the tangent to the squared current at the initial point. This is equivalent to the curve represented at Fig. 4a, which is clear that do not fits well. It is worth mentioning that similar results are reached by using the apparent power through the line instead of the current amplitude.

B. DISCUSSION

From the previous study, it is concluded that using only one sensitivity matrix to relate control variables to voltages at demand nodes leads to results with small errors.

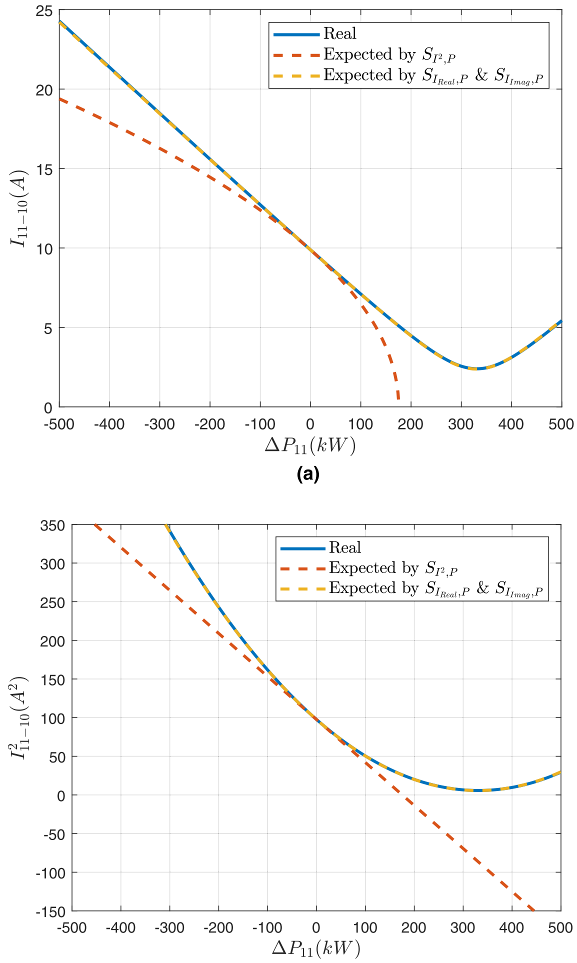

FIGURE 4. Current through line 11 - 10 and the corresponding approximations with respect to actions on the active power injected at node 11 in the MV system. (a) Current amplitude, (b) Squared current amplitude.

Similarly, using only one sensitivity matrix to relate control variables to reactive power of generators works properly, although it results in higher errors. In contrast, the amplitude of the current through lines and transformers presents controversial results.

On the one hand, adequate results are reached by the classical formulation if the line or transformer is highly loaded, and the control action do not affect significantly the current through the transformer. Then, the current amplitude will be far from zero, the phasor current will not change its quadrant and its tangent will approximate the function properly. This is the case depicted in Fig. 5.

On the other hand, the classical approach does not fit properly the current in case lines or transformers were relatively unloaded. As depicted in Fig. 4 and addressed in the previous section, the slope varies significantly close to the vertex and changes its sign because the current amplitude always remains positive.

In that sense, the error associated to the sensitivity matrices for the current through lines and transformers is unacceptable

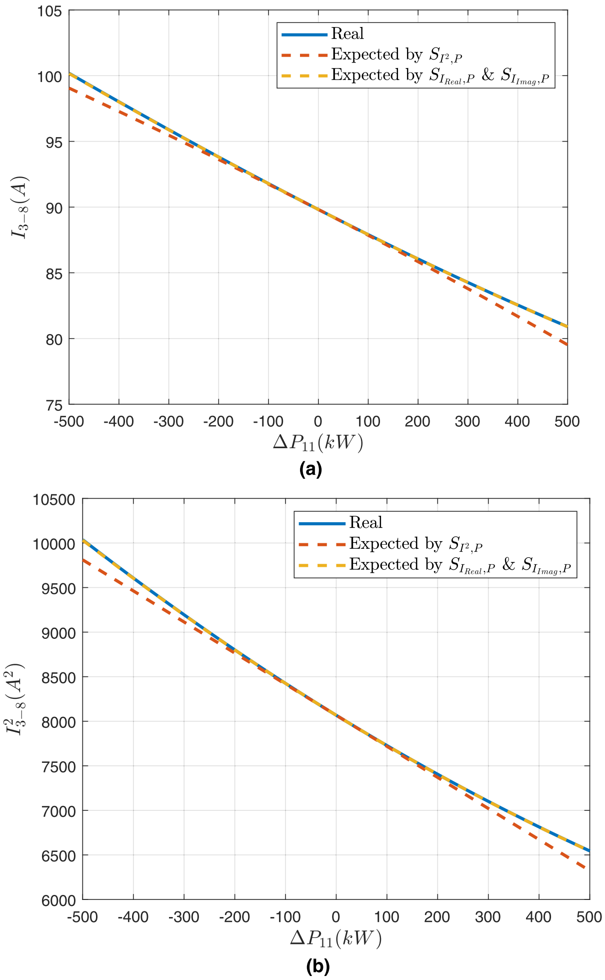

FIGURE 5. Current through line 3 – 8 and the corresponding approximations with respect to actions on the active power injected at node 11 in the MV system. (a) Current amplitude, (b) Squared current amplitude.

under certain conditions. To tackle this problem, a novel formulation is proposed in Section 4, which make it possible to fit the real curve accurately and follow considerable changes in the slope.

IV. ALTERNATIVE FORMULATION TO LINEARIZE THE CURRENT THROUGH LINES AND TRANSFORMERS

In order to linearize the current through lines and transformers, a novel formulation is proposed. The most common approach is to compute the sensitivity matrix directly with respect to the magnitude studied. In this study, the objective is to consider the current through lines and transformers to avoid congestions and, consequently, the current amplitude was used directly. However, the phasor current is compound of two terms, namely the real and imaginary component, whose associated sensitivity matrices can also be computed.

In this way, the total squared current variation can be calculated as follows for one line or transformer,

$$\Delta I^2 = I^2_{Final} - I^2_{Initial} \tag{24}$$

TABLE 4. Relative errors (%) of the current through lines and transformers by using the novel formulation (26): (a) MV system, and (b) LV system.

(A)

		Load level			
		25 %	*50 %*	*75 %*	*100 %*
P	***Max***	0.8	1.5	2.4	2.5
	Mean	<0.01	*<0.1*	*<0.1*	*<0.1*
$\boldsymbol{Q_D}$	***Max***	*<0.1*	*<0.1*	*<0.1*	*<0.1*
	Mean	<0.001	<0.001	<0.001	<0.01
t	***Max***	3.3	5.4	7.6	10.0
	Mean	0.3	0.4	0.5	0.7
$\boldsymbol{V_G}$	***Max***	8.0	7.8	7.6	8.5
	Mean	1.3	1.3	1.2	1.0

(B)

		Load level			
		25 %	*50 %*	*75 %*	*100 %*
P	***Max***	*1.4*	*2.8*	*4.5*	*6.2*
	Mean	*0.1*	*0.1*	*0.2*	*0.3*
$\boldsymbol{Q_D}$	***Max***	*0.3*	*0.7*	*1.1*	*1.4*
	Mean	*<0.01*	*<0.1*	*<0.1*	*<0.1*
$\boldsymbol{V_G}$	***Max***	*0.4*	*0.5*	*0.6*	*0.7*
	Mean	*0.1*	*0.2*	*0.2*	*0.2*

where I^2_{Final} is the squared current through a line or transformer after a control action and $I^2_{Initial}$ the initial value.

Considering the real and imaginary components along with the corresponding increases, (24) is rewritten as

$$\Delta I^2 = (I_{Real} + \Delta I_{Real})^2 + \left(I_{Imag} + \Delta I_{Imag}\right)^2 - I^2_{Real} - I^2_{Imag} \tag{25}$$

where I_{Real} and I_{Imag} refer to the real and imaginary components of the current phasor at the initial state, respectively, and ΔI_{Real} and ΔI_{Imag} are the increase in the real and imaginary component of the current phasor, respectively.

Finally, by using the corresponding sensitivities to estimate such increases, the total squared current variation can be calculated as,

$$\Delta I^2 = \left(S^2_{I_{Real},u} + S^2_{I_{Imag},u}\right)\Delta u^2 + 2\left(S_{I_{Real},u} I_{Real} + S_{I_{Imag},u} I_{Imag}\right)\Delta u \tag{26}$$

where Δu is the variation of the control considered, whereas $S_{I_{Real},u}$ and $S_{I_{Imag},u}$ the sensitivity matrices that relate the control variable u with the real and imaginary components of the current phasor at the initial state, respectively.

The new expression is quadratic and allows to fit accurately to the real curve. In fact, the second derivative is always positive and thus the curve is convex. This follows the behavior of the current amplitude closely as shown in Fig. 4 and 5 despite the wide range of the active power variation. The new approximation is depicted in yellow and almost coincide to the real curve.

Following the same reasoning as in section II, the sensitivity matrices that model control variables with respect to the real and imaginary component of the current phasor are calculated. The resulting expressions for I_{Real} are:

$$S_{I_{Real},Q_D} = \left\{ \frac{\partial I_{Real}}{\partial V_D} - \frac{\partial I_{Real}}{\partial \theta} \left[\frac{\partial P}{\partial \theta} \right]^{-1} \frac{\partial P}{\partial V_D} \right\} S_{V_D,Q_D} \quad (27)$$

$$S_{I_{Real},P} = \frac{\partial I_{Real}}{\partial \theta} \left[\frac{\partial P}{\partial \theta} \right]^{-1} - \frac{\partial I_{Real}}{\partial \theta} \left[\frac{\partial P}{\partial \theta} \right]^{-1} \frac{\partial P}{\partial V_D} S_{V_D,P} + \frac{\partial I_{Real}}{\partial V_D} S_{V_D,P} \quad (28)$$

$$S_{I_{Real},V_G} = -\frac{\partial I_{Real}}{\partial \theta} \left[\frac{\partial P}{\partial \theta} \right]^{-1} \frac{\partial P}{\partial V_D} S_{V_D,V_G} + \frac{\partial I_{Real}}{\partial V_G} - \frac{\partial I_{Real}}{\partial \theta} \left[\frac{\partial P}{\partial \theta} \right]^{-1} \frac{\partial P}{\partial V_G} + \frac{\partial I_{Real}}{\partial V_D} S_{V_D,V_G} \quad (29)$$

$$S_{I_{Real},t} = -\frac{\partial I_{Real}}{\partial \theta} \left[\frac{\partial P}{\partial \theta} \right]^{-1} \frac{\partial P}{\partial V_D} S_{V_D,t} + \frac{\partial I_{Real}}{\partial t} - \frac{\partial I_{Real}}{\partial \theta} \left[\frac{\partial P}{\partial \theta} \right]^{-1} \frac{\partial P}{\partial t} + \frac{\partial I_{Real}}{\partial V_D} S_{V_D,t} \quad (30)$$

Regarding the sensitivity matrices for I_{Imag}:

$$S_{I_{Imag},Q_D} = \left\{ \frac{\partial I_{Imag}}{\partial V_D} - \frac{\partial I_{Imag}}{\partial \theta} \left[\frac{\partial P}{\partial \theta} \right]^{-1} \frac{\partial P}{\partial V_D} \right\} S_{V_D,Q_D} \quad (31)$$

$$S_{I_{Imag},P} = \frac{\partial I_{Imag}}{\partial \theta} \left[\frac{\partial P}{\partial \theta} \right]^{-1} - \frac{\partial I_{Imag}}{\partial \theta} \left[\frac{\partial P}{\partial \theta} \right]^{-1} \frac{\partial P}{\partial V_D} S_{V_D,P} + \frac{\partial I_{Imag}}{\partial V_D} S_{V_D,P} \quad (32)$$

$$S_{I_{Imag},V_G} = -\frac{\partial I_{Imag}}{\partial \theta} \left[\frac{\partial P}{\partial \theta} \right]^{-1} \frac{\partial P}{\partial V_D} S_{V_D,V_G} + \frac{\partial I_{Imag}}{\partial V_G} - \frac{\partial I_{Imag}}{\partial \theta} \left[\frac{\partial P}{\partial \theta} \right]^{-1} \frac{\partial P}{\partial V_G} + \frac{\partial I_{Imag}}{\partial V_D} S_{V_D,V_G} \quad (33)$$

$$S_{I_{Imag},t} = -\frac{\partial I_{Imag}}{\partial \theta} \left[\frac{\partial P}{\partial \theta} \right]^{-1} \frac{\partial P}{\partial V_D} S_{V_D,t} + \frac{\partial I_{Imag}}{\partial t} - \frac{\partial I_{Imag}}{\partial \theta} \left[\frac{\partial P}{\partial \theta} \right]^{-1} \frac{\partial P}{\partial t} + \frac{\partial I_{Imag}}{\partial V_D} S_{V_D,t} \quad (34)$$

In this way, the results obtained by using the novel formulation (26) instead of relating the current amplitude directly to the control variable are much better. Regarding the previous example, the error associated to the current through the line $11 - 10$ is significantly reduced from 87 % to 0.15 % in the proposed formulation. Table 4 summarizes the results provided by this formulation for the current through lines and transformers. Compared with the results using the classical formulation (Table 3), both mean and maximum errors are reduced. The highest improvement comes from V_G when load level is 50 %. Whereas the maximum error using the classical formulation is 99.1 %, the proposed formulation leads to 0.5 %.

The novel formulation allows to consider lightly loaded lines and transformers and approximates its behavior properly. Although two sensitivity matrices are required instead of one, it will allow to reuse methodologies that only consider voltage to correct congestions within the lines and transformers of the system as well.

V. CONCLUSION

This paper analyzes the error associated to several sensitivities considering a wide range of control variables to test the adequacy of this tool to approximate electrical magnitudes. A novel formulation is also proposed that allows to extend the use of sensitivities to manage congestions through lines and transformers. In this way, it is enabled to reuse the large number of methods focused on solving voltage problems, estimating the allowable RES penetration, etc., to include congestions as well.

The initial error analysis demonstrates the difficulty of forecasting the errors associated to sensitivities and obtaining analytical expressions. The main reason is the large number of parameters that depend on the type and state of the system. A quantitative analysis is then performed to provide insight into the magnitude of the associated errors by studying two representative distribution networks. It reveals that the sensitivities regarding voltage at demand nodes and reactive power of generators works properly. However, the sensitivities for the current amplitude used to manage congestions leads to unacceptable results. A new approach is proposed based on the sensitivities that relate the real and imaginary components of the current phasor to the available control. The novel formulation results in an accurate approximation that follows the behavior of the current amplitude closely.

To sum up, this paper confirms the adequacy of sensitivities to forecast electrical magnitudes with respect to a wide range of control actions. The sensitivities related to voltages stand out because of its accuracy, whereas control actions could be limited to avoid excessive errors in case the reactive power of generators is considered. Finally, the novel approach allows to estimate closely the behavior of the current amplitude through lines and transformers, and thus also consider congestions.

REFERENCES

[1] International Energy Agency, Paris, France. (2018). *World Energy Outlook 2018*. [Online]. Available: https://www.iea.org/reports/world-energy-outlook-2018

[2] *Sustainable Development Goals*. Accessed: Mar. 16, 2021. [Online]. Available: https://www.un.org/sustainabledevelopment/en/

[3] *Directive 2009/28/EC of the European Parliament and of the Council of 23 April 2009 on the Promotion of the Use of Energy From Renewable Sources and Amending and Subsequently Repealing Directives 2001/77/EC and 2003/30 2009*, Official J. Eur. Union, Luxembourg City, Luxembourg, 2009.

[4] *Directive 2009/29/EC of the European Parliament and of the Council of 23 April 2009 Amending Directive 2003/87/EC So as to Improve and Extend the Greenhouse Gas Emission Allowance Trading Scheme of the Community*, Official J. Eur. Union, Luxembourg City, Luxembourg, 2009.

[5] European Union, Publications Office of the European Union, Luxembourg. (2012). *Energy Roadmap 2050*, doi: 10.2833/10759.

[6] F. J. Zarco-Soto, J. L. Martínez-Ramos, and P. J. Zarco-Periñán, "Voltage control in active distribution networks," in *Power Quality in Modern Power Systems*, P. Sanjeevikumar, C. Sharmeela, J. B. Holm-Nielsen, and P. Sivaraman, Eds., 1st ed. London, U.K.: Academic, 2020, pp. 193–217, doi: 10.1016/B978-0-12-823346-7.00003-7.

[7] P. P. Barker and R. W. D. Mello, "Determining the impact of distributed generation on power systems. I. Radial distribution systems," in *Proc. Power Eng. Soc. Summer Meeting*, Seattle, WA, USA, vol. 3, Jul. 2000, pp. 1645–1656, doi: 10.1109/PESS.2000.868775.

[8] S.-E. Razavi, E. Rahimi, M. S. Javadi, A. E. Nezhad, M. Lotfi, M. Shafie-khah, and J. P. S. Catalão, ''Impact of distributed generation on protection and voltage regulation of distribution systems: A review,'' *Renew. Sustain. Energy Rev.*, vol. 105, pp. 157–167, May 2019, doi: 10.1016/j.rser.2019.01.050.

[9] M. B. Buchholz and Z. Styczynski, ''The three pillars of smart distribution, pillar 1: Automation and remote control of local distribution networks,'' in *Smart Grids—Fundamentals and Technologies in Electricity Networks*. New York, NY, USA: Springer, 2014, pp. 225–275, doi: 10.1007/978-3-642-45120-1.

[10] V. A. Evangelopoulos, I. I. Avramidis, and P. S. Georgilakis, ''Flexibility services management under uncertainties for power distribution systems: Stochastic scheduling and predictive real-time dispatch,'' *IEEE Access*, vol. 8, pp. 38855–38871, 2020, doi: 10.1109/ACCESS.2020.2975663.

[11] H. Gerard, E. I. R. Puente, and D. Six, ''Coordination between transmission and distribution system operators in the electricity sector: A conceptual framework,'' *Utilities Policy*, vol. 50, pp. 40–48, Feb. 2018, doi: 10.1016/j.jup.2017.09.011.

[12] X. Ke, N. Samaan, J. Holzer, R. Huang, B. Vyakaranam, M. Vallem, M. Elizondo, N. Lu, X. Zhu, B. Werts, Q. Nguyen, A. Huang, and Y. V. Makarov, ''Coordinative real-time sub-transmission volt–var control for reactive power regulation between transmission and distribution systems,'' *IET Gener., Transmiss. Distrib.*, vol. 13, no. 11, pp. 2006–2014, Jun. 2019, doi: 10.1049/iet-gtd.2018.5850.

[13] J. Silva, J. Sumaili, R. J. Bessa, L. Seca, M. A. Matos, V. Miranda, M. Caujolle, B. Goncer, and M. Sebastian-Viana, ''Estimating the active and reactive power flexibility area at the TSO-DSO interface,'' *IEEE Trans. Power Syst.*, vol. 33, no. 5, pp. 4741–4750, Sep. 2018, doi: 10.1109/TPWRS.2018.2805765.

[14] Z. Rafique, H. M. Khalid, and S. M. Muyeen, ''Communication systems in distributed generation: A bibliographical review and frameworks,'' *IEEE Access*, vol. 8, pp. 207226–207239, 2020, doi: 10.1109/ACCESS.2020.3037196.

[15] T. R. F. Mendonca and T. C. Green, ''Distributed active network management based on locally estimated voltage sensitivity,'' *IEEE Access*, vol. 7, pp. 105173–105185, 2019, doi: 10.1109/ACCESS.2019.2931955.

[16] J. L. Martinez-Ramos, F. J. Zarco-Soto, A. Marano-Marcolini, P. J. Zarco-Perinan, and A. L. Trigo-Garcia, ''Coordination of distributed energy resources to solve voltage problems in distribution networks,'' in *Proc. Int. Conf. Smart Energy Syst. Technol. (SEST)*, Sep. 2018, pp. 1–6, doi: 10.1109/SEST.2018.8495842.

[17] R. A. Jabr and I. Dzafic, ''Sensitivity-based discrete coordinate-descent for Volt/VAr control in distribution networks,'' *IEEE Trans. Power Syst.*, vol. 31, no. 6, pp. 4670–4678, Nov. 2016, doi: 10.1109/TPWRS.2015.2512103.

[18] F. Tamp and P. Ciufo, ''A sensitivity analysis toolkit for the simplification of MV distribution network voltage management,'' *IEEE Trans. Smart Grid*, vol. 5, no. 2, pp. 559–568, Mar. 2014, doi: 10.1109/TSG.2014.2300146.

[19] V. Calderaro, V. Galdi, G. Massa, and A. Piccolo, ''Distributed generation and local voltage regulation: An approach based on sensitivity analysis,'' in *Proc. 2nd IEEE PES Int. Conf. Exhib. Innov. Smart Grid Technol.*, Dec. 2011, pp. 1–8, doi: 10.1109/ISGTEurope.2011.6162803.

[20] H. M. Ayres, W. Freitas, M. C. De Almeida, and L. C. P. D. Silva, ''Method for determining the maximum allowable penetration level of distributed generation without steady-state voltage violations,'' *IET Gener., Transmiss. Distrib.*, vol. 4, no. 4, pp. 495–508, 2010, doi: 10.1049/iet-gtd.2009.0317.

[21] S. Huang, Q. Wu, Z. Liu, and A. H. Nielsen, ''Review of congestion management methods for distribution networks with high penetration of distributed energy resources,'' in *Proc. IEEE PES Innov. Smart Grid Technol., Eur.*, Oct. 2014, pp. 1–6, doi: 10.1109/ISGTEurope.2014.7028811.

[22] I. Bilibin, F. Capitanescu, and J. Sachau, ''Overloads management in active radial distribution systems: An optimization approach including network switching,'' in *Proc. IEEE Grenoble Conf.*, Jun. 2013, pp. 1–5, doi: 10.1109/PTC.2013.6652327.

[23] W. Liu, Q. Wu, F. Wen, and J. Ostergaard, ''Day-ahead congestion management in distribution systems through household demand response and distribution congestion prices,'' *IEEE Trans. Smart Grid*, vol. 5, no. 6, pp. 2739–2747, Nov. 2014, doi: 10.1109/TSG.2014.2336093.

[24] P. Purey, ''A look ahead load shed strategy for line overload alleviation based on the sensitivity of a severity index incorporating distributed generations,'' *IUP J. Electr. Electron. Eng.*, vol. 11, no. 2, pp. 53–71, 2018.

[25] J. Rocabert, A. Luna, F. Blaabjerg, and P. Rodríguez, ''Control of power converters in AC microgrids,'' *IEEE Trans. Power Electron.*, vol. 27, no. 11, pp. 4734–4749, Nov. 2012, doi: 10.1109/TPEL.2012.2199334.

[26] D. H. Vu, K. M. Muttaqi, A. P. Agalgaonkar, and A. Bouzerdoum, ''Customer reward-based demand response program to improve demand elasticity and minimise financial risk during price spikes,'' *IET Gener., Transmiss. Distrib.*, vol. 12, no. 15, pp. 3764–3771, Aug. 2018, doi: 10.1049/iet-gtd.2017.2037.

[27] P. Palensky and D. Dietrich, ''Demand side management: Demand response, intelligent energy systems, and smart loads,'' *IEEE Trans. Ind. Informat.*, vol. 7, no. 3, pp. 381–388, Aug. 2011, doi: 10.1109/TII.2011.2158841.

[28] Y. Zheng, S. Niu, Y. Shang, Z. Shao, and L. Jian, ''Integrating plug-in electric vehicles into power grids: A comprehensive review on power interaction mode, scheduling methodology and mathematical foundation,'' *Renew. Sustain. Energy Rev.*, vol. 112, pp. 424–439, Sep. 2019, doi: 10.1016/j.rser.2019.05.059.

[29] A. Gómez-Expósito and F. L. Alvarado, ''Load flow,'' in *Electric Energy Systems: Analysis and Operation*, A. Gomez-Exposito, A. Conejo, and C. Cañizares, Eds., 2nd ed. Boca Raton, FL: CRC Press, 2018, pp. 99–132, doi: 10.1201/9781420007275.

[30] K. Rudion, A. Orths, Z. A. Styczynski, and K. Strunz, ''Design of benchmark of medium voltage distribution network for investigation of DG integration,'' in *Proc. IEEE Power Eng. Soc. Gen. Meeting*, Montreal, QC, Canada, Jun. 2006, p. 6, doi: 10.1109/PES.2006.1709447.

[31] *Benchmark Systems for Network Integration of Renewable and Distributed Energy Resources*, Standard CIGRE Task Force C6.04.02, 2013.

[32] A. Gómez-Expósito, J. L. Martínez-Ramos, J. L. Ruiz-Macías, and Y. Cuéllar-Salinas, ''Sensitivity-based reactive power control for voltage profile improvement,'' *IEEE Trans. Power Syst.*, vol. 8, no. 3, pp. 937–945, Aug. 1993, doi: 10.1109/59.260908.

[33] J. L. Martínez-Ramos, A. Gómez-Expósito, J. Cortés-Cerezo, E. Méndez-Ruiz, and Y. Cuéllar-Salinas, ''A hybrid tool to assist the operator in reactive power/voltage control and optimization,'' *IEEE Trans. Power Syst.*, vol. 10, no. 2, pp. 760–768, May 1995, doi: 10.1109/59.387914.

[34] A. Gómez, J. L. Martínez, A. Cabrera, J. Cortés, J. J. Mateos, J. L. Tuiz, E. Méndez, Y. Cuéllar, and A. Hurtado, ''Benefits of using an operational tool for reactive power scheduling,'' in *Proc. 12th Power Syst. Comput. Conf.*, 1996, pp. 837–843.

FCO. JAVIER ZARCO-SOTO was born in Seville, Spain. He received the M.Sc. degree in industrial engineering, in 2019, and the M.Sc. degree in electrical energy systems, in 2020. He is currently pursuing the Ph.D. degree in electrical engineering with the University of Seville. Since 2019, he has been with the Department of Electrical Engineering, University of Seville. His research interests include power system operation and control, integration of renewable energy sources, and power electronics.

JOSÉ L. MARTÍNEZ-RAMOS (Senior Member, IEEE) was born in Dos Hermanas, Spain, in 1964. He received the Ph.D. degree in electrical engineering from the University of Seville, Seville, Spain, in 1994. Since 1990, he has been with the Department of Electrical Engineering of the University of Seville, where he is currently a Full Professor. His research interests include active and reactive power optimization, power system planning, analysis and control, and electricity markets.

PEDRO J. ZARCO-PERIÑÁN was born in Seville, Spain. He received the Ph.D. degree in electrical engineering from the University of Seville and the M.B.A. degree from Deusto University. Since 1989, he has been with the Department of Electrical Engineering, University of Seville, where he is currently an Assistant Professor. He has also worked in different electricity companies and has been a member of technical committees for the development of standards and regulations for the Spanish electricity sector. His research interests include the development and maintenance of facilities, optimization of energy systems, and power system planning.